

A 4×4 Tin Oxide Gas Sensor Array with On-chip Signal Pre-processing

Bin Guo, Amine Bermak, Philip C. H. Chan

Electronic and Computer Engineering Department, Hong Kong University of Science and Technology
Clear Water Bay, Kowloon, Hong Kong. Email: guobin@ust.hk

Gui-Zhen Yan

Institute of Microelectronics, Peking University, Beijing, China.

Abstract—This paper presents a monolithic 4×4 tin oxide gas sensor array together with on-chip multiplexing and differential read-out circuitry. In contrast to the conventional voltage divider read-out technique, a novel differential read-out circuit (DRC) for tin oxide gas sensors is proposed. The output of the DRC is simply proportional to the difference between the voltage on the two electrodes of the sensor but not to the transistor parameters such as mobility and threshold voltage, neither to the supply voltage. A robust fabrication process focusing on the integration of the CMOS circuitry and the MEMS structures is described. The monolithic sensor array and its processing circuitry have been implemented in our in-house 5 μm process. Experimental results showed good linearity at the output of the DRC for a wide range of sensor resistance variation (over 20 MΩ). Results also show good thermal characteristic leading to only 15.5 mW power consumption for 300 °C operating temperature.

Keywords: Tin Oxide, Gas Sensor Array, Differential Readout, Monolithic Integration

I. INTRODUCTION

THE detection and discrimination of gases using micro-electronic gas sensor array is required in various industry and domestic applications, such as automobiles, safety, indoor air quality, medicine and food industry [1]. SnO₂-based gas sensing film is commonly used for such applications because of a number of advantages including cost effective, high sensitivity to various gases and relative compatibility with standard CMOS fabrication processes. Typically tin oxide gas sensors are preheated to facilitate the sensor's reaction before being exposed to an analyte gas, by the micro-machined micro-hotplate (MHP), for the sensing mechanism is based upon a chemical reaction at the surface of the sensing film. After exposure to the target gas, the resistance of the sensor is affected.

SnO₂-based gas sensing film shows high response to a large variety of target gases but low level of selectivity to a given target gas. This phenomenon is widely exhibited in the animal and human biological olfactory systems [2]. Inspired from biological systems, a number of researchers are currently interested in improving the overall selectivity by designing a large number of sensors [3]. Silicon-based gas sensors have the potential to produce low cost and low power devices for

the growing consumer market [4]. The micro-machined SnO₂-based sensor array [5], [6] is relatively attractive for integration with on chip CMOS circuitry. Conventional SnO₂-based gas sensor relies on voltage divider read-out strategy, which is hardly implemented on-chip and presents the drawback of being vulnerable to common mode noise. This paper presents a differential read-out circuit (DRC), which is integrated together with a 4×4 gas sensor array. The gain of the differential read-out circuit can be adjusted in order to tune the sensitivity of the sensor.

At the sensor level, although different research groups [5], [6], [7], [8], [9] have reported the fabrication of array-based tin oxide gas sensors, large dimension arrays (4×4 or above) based on MHP remain a real challenge. This is mainly due to difficulties in manufacturing large number of sensing films on the same die, which leads to reduced yield. In this paper, the design and fabrication process of a 4×4 gas sensor array with MHP structures using surface micro-machining process suitable for large dimension arrays is demonstrated.

II. SENSOR FABRICATION AND INTEGRATION

The cross-sectional view of the gas sensor is shown in Figure 1.a. The top view of the fabricated MHP with the micro heater and the electrodes is shown in Figure 1.b. The gas sensor element uses a surface micro-machined structure. The base of the MHP membrane is formed using 800 nm densified Low Temperature Oxide (LTO), 1 μm low stress silicon nitride (Si₃N₄) and 2 μm LTO (O/N/O) multi-layer. The MHP is at the center of the sensor cell and has a dimension of 190×190 μm². A 3 μm air gap between the hotplate membrane and the SiO₂ underneath the membrane is formed by etching a sacrificial polysilicon layer. There are four etching windows used to facilitate the removal of the sacrificial polysilicon.

The serpentine shape Platinum (Pt) layer, at the center of the MHP, defines the micro heater. The tin oxide sensing film is deposited on top of the micro-heater while the sensor electrodes are formed following the sensing film. The heater and electrodes are realized using a layer of 100 nm Pt and a 20 nm Tungsten-Titanium (TiW) used as the adhesion layer. The surface micro-machined process, which will be described later, ensures the integrity of the sensor array. The SnO₂ sensing film is deposited onto the MHP using sputtering method. The sensor signal is deduced from the resistance variation across

This work was sponsored by (HKUST 6162/04E) from the Research Grant Council of Hong Kong.

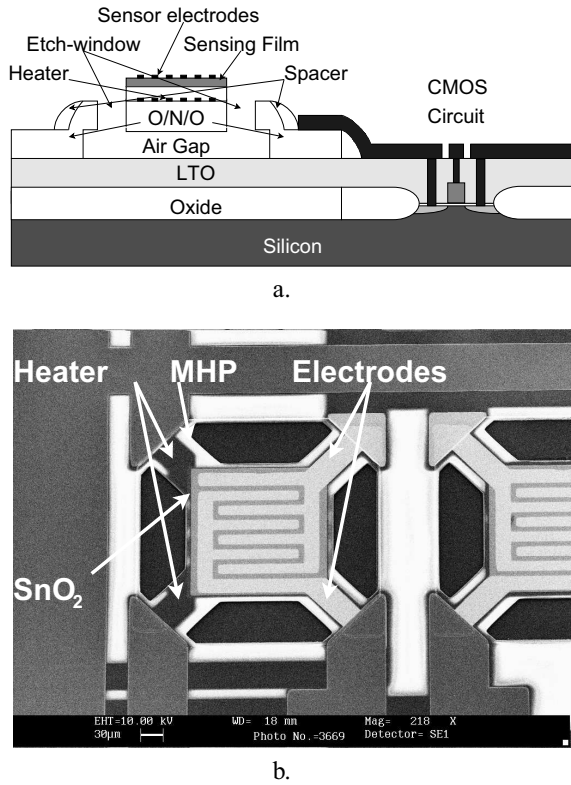


Fig. 1. (a) The structure of the sensor element. (b) The SEM picture of the sensor element.

the two Pt electrodes. The general mechanism for gas detection using tin oxide sensors is based on sensing a change in the resistance of the sensor when exposed to an analyte. The change in resistance is due to irreversible reactions between the analyte and the oxygen-derived compound such as O^- , O_2^- , and O^{2-} on the tin oxide surface [10].

The monolithic tin oxide gas sensor array was designed and fabricated using our in-house $5 \mu\text{m}$ 1-metal, 1-poly CMOS process. Unlike conventional post-processing technique, the proposed process forms the CMOS devices first followed by the MEMS structure. Once the devices and the MEMS structures are finalized, the interconnection layers are deposited as the last step. This process sequence permits to avoid damaging the Aluminum (Al) interconnect, when applying high temperature annealing required for the realization of the tin oxide gas sensing films. The details of all the steps are reported in Table I.

The steps shown in Table I can be commonly found in standard IC fabrication process, except for steps 11 and 13 particularly used for the sensor fabrication. Step 11 is required for spacer formation of the MHP membrane to strengthen the MHP structure and facilitate the Al interconnections across the MEMS structure and the CMOS circuit. Step 13 is required for the formation of the Pt heaters and the electrodes by sputtering and lift-off process, which is carried out after the release of the MHP structure.

TABLE I
PROPOSED CMOS-MEMS INTEGRATION PROCESS.

Step	Mask	Process
1	Nwell	Nwell formation
2	Active	Field implant, initial oxidation
3	N/A	Threshold implant
4	N/A	Gate oxidation
5	Poly	Polysilicon gate formation
6	Pimp	PMOS implantation
7	Nimp	NMOS implantation
8	N/A	LTO deposition
9	Sacri	Sacrificial polysilicon formation
10	N/A	Oxide and Nitride deposition
11	Step	Spacer oxide deposition and etch
12	Etch	Etch window open
13	Pt	Platinum heater
14	N/A	PECVD oxide
15	Pt-Pt	Contact holes for Pt electrodes
16	SnO	SnO ₂ film formation
17	N/A	SnO ₂ anneal
18	Electrode	Pt electrodes
19	Cont	Contact hole open
20	Metal	Al deposition and pattern

III. ON-CHIP PRE-PROCESSING CIRCUITS

A. Read-out circuit: Analysis and Simulation

The proposed differential read-out circuit is shown in Figure 2.a together with the expected output response shown in Figure 2.b.

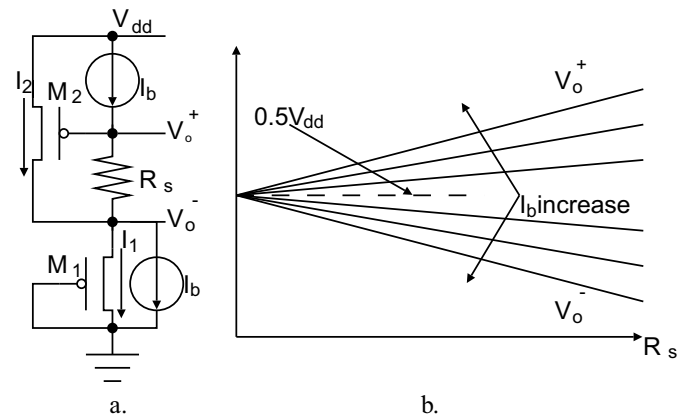


Fig. 2. (a) Proposed differential readout scheme. (b) Output response seen at the two sensor's terminals.

The voltage difference across the sensor's resistance R_s can be expressed by

$$(V_o^+) - (V_o^-) = I_b \times R_s \quad (1)$$

Where V_o^+ and V_o^- are the positive and negative differential outputs, respectively. I_b is the bias current applied to the sensor. Assuming that transistor M_2 is operating in the saturation region and constituting a ratioed inverter, with M_1 being the load, therefore we can write:

$$V_{dd} - (V_o^+) - V_{th} = \sqrt{\frac{2 \times I_2}{C_{ox} \mu \left(\frac{W}{L}\right)_2}} \quad (2)$$

Where V_{dd} is the supply voltage, V_{th} is the threshold voltage of the PMOS transistors, C_{ox} and μ are the gate capacitance and the mobility, respectively. I_2 is the current passing through M_2 , which is set equal to the current passing through transistor M_1 ($I_1 = I_2$) by adding another current source equals to the bias I_b and placed in parallel with transistor M_1 . We can therefore write:

$$(V_o^-) - V_{th} = \sqrt{\frac{2 \times I_2}{C_{ox}\mu\left(\frac{W}{L}\right)_1}} \quad (3)$$

By setting $\left(\frac{W}{L}\right)_1 = \left(\frac{W}{L}\right)_2$, we can deduce:

$$V_{dd} = (V_o^+) + (V_o^-) \quad (4)$$

From Eq. (4) one can note that the sum of V_o^+ and V_o^- is equal to V_{dd} regardless of R_s and I_b values. Using Eq. (1) and Eq. (4), we obtain:

$$(V_o^+) = \frac{V_{dd}}{2} + \frac{I_b \times R_s}{2} \quad (5)$$

$$(V_o^-) = \frac{V_{dd}}{2} - \frac{I_b \times R_s}{2} \quad (6)$$

One can see from equations Eq. (5) and Eq. (6) that $V_{dd}/2$ is the common mode component and $I_b/2$ is the differential gain, while R_s is the input resistance variable. The approximated output voltage does not depend on any transistor parameters such as mobility or threshold voltage, which indicates that the circuit can compensate for first order undesirable process variations. In addition, the differential output is independent of V_{dd} and hence supply voltage rejection property is also inherent in this design.

The transistor level schematic of the DRC is shown in Figure 3.a.

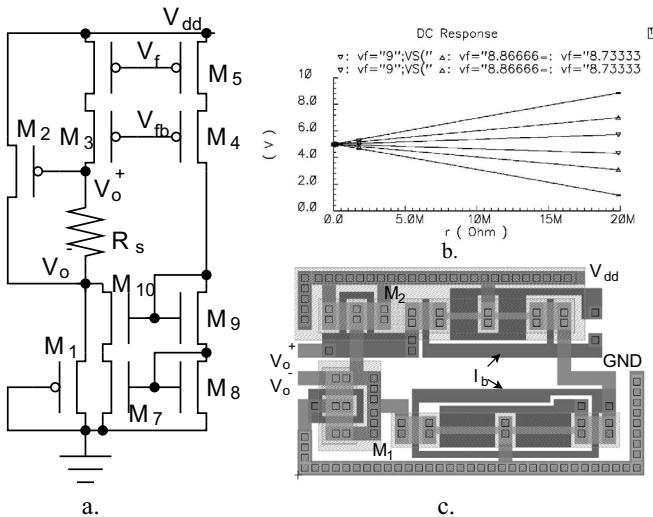


Fig. 3. (a) Schematic of the proposed differential readout circuit. (b) Simulated result. (c) Layout.

The two I_b current sources are implemented using two Cascode current mirrors. Totally only 10 transistors are needed for the DRC implementation. Figure 3.b illustrates the simulation results of the DRC circuit for different biasing currents. The

output response illustrated in Fig 3.a and described through the mathematical expression is validated in our simulation results. The sensitivity is increased by increasing the bias current I_b as this will result in a larger differential output signal ($V_o^+ - V_o^-$). Figure 3.c illustrates the layout of the DRC.

B. Multiplexing circuits

The response time of tin-oxide gas sensors is in the range of few to hundreds of seconds depending on the sensing film material, the target gas and the operating temperature [6]. Time multiplexing read-out techniques are therefore preferable in order to utilize more effectively the available hardware resources and to lower the overall cost and power consumption. The 4×4 sensor array is multiplexed using a set of column and row decoders as well as analog switches. There are totally 16 column switches and 4 row switches, which are implemented using NMOS transistors. The multiplexing circuit has been implemented in the same die. The schematic of the 2-4 decoder in the multiplexer and its output curves are shown in Figure 4.a and b, respectively.

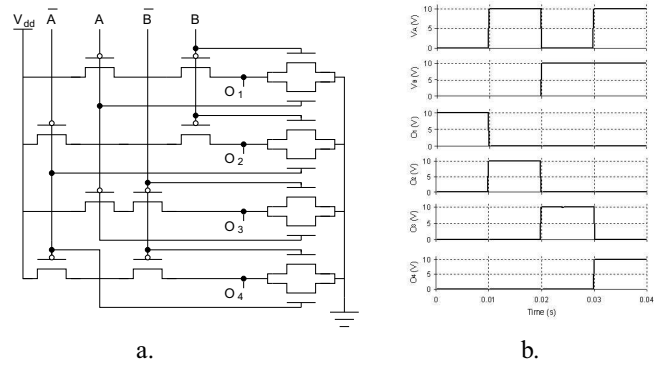


Fig. 4. (a) Schematic of the proposed 2-4 decoder. (b) Measurement output curves.

IV. MEASUREMENT RESULTS AND DISCUSSION

The micrograph of the fabricated monolithic gas sensor array and its pre-processing circuitry is shown in Figure 5. The sensor array consists of 16 micro-hotplate elements and is multiplexed by on chip decoders and analog switches. The 4×4 gas sensor array is fabricated using the process described in the previous section. The experimentally measured thermal response of the fabricated MHP is shown in Figure 6. The thermal efficiency of the MHP was measured at about $18.2^\circ\text{C}/\text{mW}$. A power consumption of only 15.5 mW is therefore required to reach a typical MHP operating temperature of 300°C . Figure 7 illustrates the measured response of the fabricated differential readout circuit. Note that a supply voltage of 10 V is used in order to ensure good dynamic and correct multiplexing of the sensor's signal. The 3 pair of curves correspond to 3 biasing currents, $I_b = 300$ nA, $1 \mu\text{A}$ and $5 \mu\text{A}$, in which the outputs are described by Eq. (5) and (6). The gain of the readout circuit is increased by increasing the biasing current, while the common mode output remains at $V_{dd}/2 = 5$ V. It is clearly shown that the sensitivity of the

read-out circuit can be modulated by tuning the bias current I_b . The measured results from the fabricated 2-4 decoder are shown in Figure 4.b with a period $T = 40$ ms. The outputs of the decoder are used to control the transmission gates used to select a sensor within the 4×4 array.

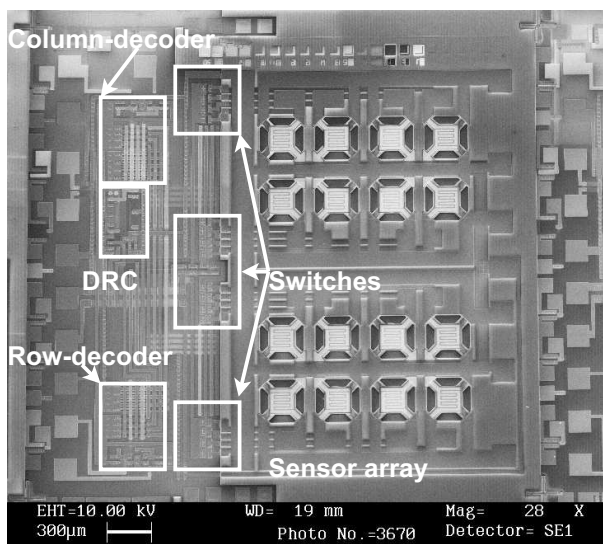


Fig. 5. Microphotograph of the fabricated monolithic integrated 4×4 tin oxide gas sensor array and its pre-processing circuits.

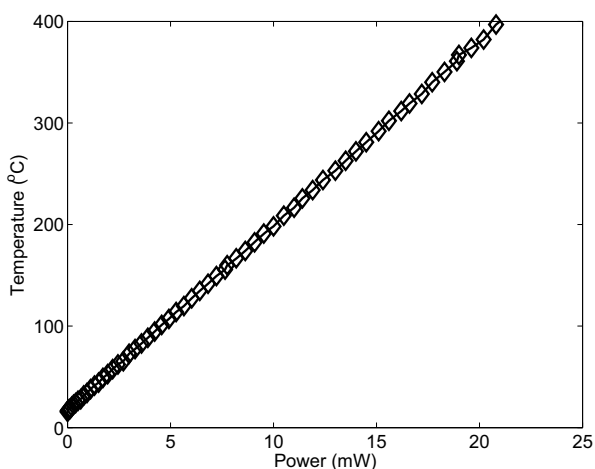


Fig. 6. Thermal response of the fabricated MHP and its corresponding power consumption.

V. CONCLUSION

This paper reports the design, fabrication and experimental test of a monolithic 4×4 tin oxide gas sensor array together with its integrated multiplexing and differential read-out circuitry. A monolithic process integrating both the sensors and the CMOS circuitry is developed. In contrast to traditional single-ended voltage dividers, a DRC circuit uses a differential read-out strategy is proposed. It was shown that the sensor's sensitivity can be calibrated by tuning the bias current of the read-out circuit. Experimental results showed good linearity

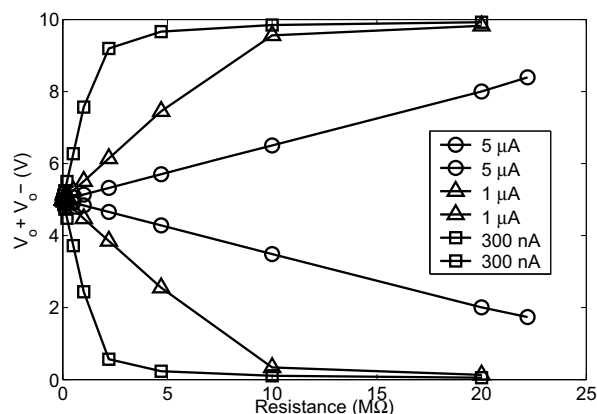


Fig. 7. Measured output signals from the fabricated DRC.

of the read-out circuit over a wide range of sensor resistance values. Measurements also demonstrated reasonable power consumption and good thermal efficiency of the micro-hotplate structure.

ACKNOWLEDGMENTS

The authors would like to acknowledge the help of Mr. Darwin Wong, Mr. Ming-Hua Shi and Mr. Siu Fai LUK during the packaging and testing of the sensor array.

REFERENCES

- [1] S. Capone, A. Forleo, L. Francioso, R. Rella, P. Siciliano, J. Spadavecchia et al., "Solid State Gas Sensors: State of the Art and Future Activities", *Journal of Optoelectronics and Advanced Materials*, Vol. 5, No. 5, 2003, pp. 1335-1348.
- [2] Rafael Castro, Mrinal Kr. Mandal, Peter Ajemba and Peter Ajemba, "An Electronic Nose for Multimedia Applications", *IEEE Transactions on Consumer Electronics*, Vol. 49, No. 4, Nov 2003, pp. 1431-1437.
- [3] P.I. Neves and J.V. Hatfield, "A new generation of integrated electronic noses", *Sensors and Actuators B*, 26-27, 1995, pp. 223-231.
- [4] W. Goepel, K.D. Schierbaum, "SnO₂ Sensors: Current Status and Future Prospects", *Sensors and Actuators B*, 26/27, 1995, pp. 1-12.
- [5] Muhammad Y. Afridi, John S. Suehle, Mona E. Zaghoul, David W. Brning, Allen R. Hefner, Richard E. Cavicchi et al., "A monolithic CMOS Microhotplate-Based Gas Sensor System", *IEEE Sensors Journal*, Vol. 2, No. 6, Dec 2002, pp. 644-655.
- [6] Sofiane Brahim-Belhouari, Amine Bermak, Minghua Shi, and Philip C. H. Chan, "Fast and Robust Gas Identification System Using an Integrated Gas Sensor Technology and Gaussian Mixture Models", *IEEE Sensors Journal*, VOL. 5, NO. 6, Dec 2005, pp. 1433-1444.
- [7] C. Can, I. Garcia, A. Gtz, L. Fonseca, E. Lora-Tamayo, M. C. Horrillo, I. Sayago, J. I. Robla, J. Rodrigo and J. Gutierrez, "Detection of gases with arrays of micromachined tin oxide gas sensors", *Sensors and Actuators B*, 65, 2000, pp. 244-246.
- [8] A. Dieguez, J.L. Merino, R. Casanova, S.A. Bota, J. Samitier, M.J. Lopez, J.A. Plaza, I. Gracia, C. Cane, "A CMOS monolithically integrated gas sensor array with electronics for temperature control and signal interfacing". *IECON 02*, Vol. 4, 5-8, Nov. 2002, pp.2727 - 2732.
- [9] U. Frey, M. Graf, S. Taschini, K.-U. KIRSTEIN, C. Hagleitner, A. Hierlemann, and H. Baltes, "A Digital CMOS Micro-Hotplate Array for Analysis of Environmentally Relevant Gases", *ESSCIRC 2004*, Sep 2004, pp. 299-302.
- [10] Keith J. Albert, Nathan S. Lewis, Caroline L. Schauer, Gregory A. Sotzing, Shannon E. Stitzel and David R. Walt, "Cross-Reactive Chemical Sensor Arrays", *Chem. Rev.*, 2000, 100, 2595-2626.